The Record-Breaking 1933 Atlantic Hurricane Season

Philip J. Klotzbach*

Department of Atmospheric Science

Colorado State University

Fort Collins CO   80523

Carl J. Schreck III

North Carolina Institute for Climate Studies, Cooperative Institute for Satellite Earth System

Studies (CISESS)

North Carolina State University

Asheville NC   28801

Gilbert P. Compo

University of Colorado

Cooperative Institute for Research in Environmental Sciences

and

National Oceanic and Atmospheric Administration

Physical Sciences Laboratory

Boulder CO   80305

1

Steven G. Bowen

Aon

Chicago IL   60601

Ethan J. Gibney

UCAR/Cooperative Programs for the Advancement of Earth System Science

San Diego, CA 92127

Eric C. J. Oliver

Department of Oceanography

Dalhousie University

Halifax NS   B3H 4R2

Michael M. Bell

Department of Atmospheric Science

Colorado State University

Fort Collins CO   80523

2

Submitted to the Bulletin of the American Meteorological Society

Date: 19 June 2020

Revised: 23 September 2020

*Corresponding author address: Philip J. Klotzbach, Department of Atmospheric Science,

Colorado State University, Fort Collins, CO 80523   email: philk@atmos.colostate.edu

Abstract

The 1933 Atlantic hurricane season was extremely active, with 20 named storms and 11 hurricanes including 6 major (Category 3+; one-minute maximum sustained winds >=96 kt) hurricanes occurring. The 1933 hurricane season also generated the most Accumulated Cyclone Energy (an integrated metric that accounts for frequency, intensity, and duration) of any Atlantic hurricane season on record. A total of 8 hurricanes tracked through the Caribbean in 1933 - the most on record. In addition, two Category 3 hurricanes made landfall in the United States just 23 hours apart: the Treasure Coast hurricane in southeast Florida followed by the Cuba-Brownsville hurricane in south Texas.

This manuscript examines large-scale atmospheric and oceanic conditions that likely led to such an active hurricane season. Extremely weak vertical wind shear was prevalent over both the Caribbean and the tropical Atlantic throughout the peak months of the hurricane season, likely in part due to a weak-to-moderate La Niña event. These favorable dynamic conditions, combined with above-normal tropical Atlantic sea surface temperatures, created a very conducive environment for hurricane formation and intensification. The Madden-Julian oscillation was relatively active during the summer and fall of 1933, providing sub-seasonal conditions that were quite favorable for tropical cyclogenesis during mid-to-late August and late September to early October. The current early June and August statistical models used by Colorado State University would have predicted a very active 1933 hurricane season. A better understanding of these extremely active historical Atlantic hurricane seasons may aid in anticipation of future hyperactive seasons.

4

Capsule Summary

The 1933 Atlantic hurricane season was extremely active, generating the most Accumulated Cyclone Energy on record. The season would have been well anticipated using current statistical seasonal forecasting models.

Keywords

5

Introduction

The 2005 North Atlantic (hereafter Atlantic) hurricane season is considered by many to be the most active Atlantic hurricane season on record, with a total of 28 named storms[1] and 15 hurricanes, including 7 major hurricanes[2] occurring (Beven et al. 2008). While 2005 currently holds the record for most named storms and hurricanes in a single season (Landsea and Franklin 2013), the record for most Accumulated Cyclone Energy (ACE) in a single season occurred more than 70 years earlier - in 1933. ACE is an integrated metric that accounts for intensity and duration of storms (Bell et al. 2000). Table 1 compares seasonal summary statistics for both hurricane seasons along with the 1981–2010 climatology currently used by NOAA. By almost any measure, both seasons rank in the top five since 1851 (when the Atlantic hurricane database began), with more than twice as much tropical cyclone (TC) activity occurring compared with what is generated in an average TC season.

The TC activity records set in 1933 are notable given that they occurred in an era prior to satellite monitoring and aircraft reconnaissance (Landsea et al. 2014). The 1933 Atlantic hurricane season has undergone reanalysis as part of the Atlantic Hurricane Database Reanalysis Project (Landsea et al. 2014). For 1933, the observed total of named storms, hurricanes, and major hurricanes changed, respectively, from 21 to 20, 10 to 11, and 5 to 6 with the reanalysis compared with the original analysis. More notably, the ACE from 1933 increased by 22% (from

---

[1] Named storms are defined to be tropical cyclones having one-minute maximum sustained winds >= 34 kt.

[2] Major hurricanes are defined to be Category 3+ hurricanes on the Saffir-Simpson Hurricane Wind Scale. These hurricanes have one-minute maximum sustained winds >= 96 kt.

6

213 to 259). While the reanalysis likely removed some uncertainties from the original analysis, there remain potential underestimates in overall levels of TC activity, especially in the eastern and central Atlantic given the relative paucity of ship traffic in available databases south of 30°N, east of 60°W between 1915–1945 as shown in Figure 2 of Vecchi and Knutson (2008). Landsea et al. (2014) noted that there was an average intensity uncertainty of 20 kt with an intensity error bias of -10 kt for TCs over the open ocean from 1886 (when the original Atlantic hurricane database began) to 1943 (when aircraft reconnaissance began). This low intensity bias likely means that 1933 generated even more ACE than currently listed.

In addition, Vecchi and Knutson (2011) estimate that ~1 hurricane per year was likely missed given the observational network of the 1930s. As was noted in Landsea et al. (2010), there has been a large increase in the number of short-lived named storms (defined as named storms lasting <=48 hr) due to observational improvements in recent years. For example, in 1933, four Atlantic named storms lasted 48 hours or less, while in 2005, eight Atlantic named storms lasted 48 hours or less. Consequently, there were probably some weak, short-lived storms that were missed in 1933 that would shrink the current difference of eight named storms between 1933 (20 named storms) and 2005 (28 named storms). Regardless of whether 1933 or 2005 generated more activity by a particular metric, both seasons were extremely active and impactful to coastal and island populations.

The 1933 Atlantic hurricane season generated 20 named storms, 11 of which became hurricanes and 6 of which became major hurricanes (Fig. 1). The season was especially active in the Caribbean, defined to extend from 10–20°N, 90–60°W. A total of 8 hurricanes tracked through

the Caribbean in 1933 — the most on record. The 1933 Atlantic hurricane season also had the shortest period of time on record between major continental US (CONUS) landfalling hurricanes — a mere 23 hours between the Treasure Coast hurricane on 4 September at 05 UTC and the Cuba-Brownsville hurricane on 5 September at 04 UTC. Figure 2a displays the US Weather Bureau map from 8am EST (13 UTC) on September 4 showing the Treasure Coast hurricane onshore with the Cuba-Brownsville hurricane bearing down on Texas. Figure 2b displays a similar representation from the NOAA-CIRES-DOE 20th Century Reanalysis version 3 (20CRv3; Slivinski et al. 2019, described in more detail in the next section) at 12 UTC on September 4.   Please see the sidebar for a discussion of how the insurance industry would likely respond to two major hurricanes making landfall in the CONUS in such rapid succession.

This study examines the historic 1933 hurricane season in detail. We investigate the large-scale atmospheric-oceanic conditions that contributed to the hyperactive season. In particular, we examine how well the current early June and August statistical models used by Colorado State University (CSU) would have anticipated the 1933 hurricane season. Improved understanding of the 1933 Atlantic hurricane season may help us better anticipate future hyperactive Atlantic seasons.

Data

Atlantic TC dataset

Atlantic TC data are calculated from HURDAT2 (Landsea and Franklin 2013). This dataset provides six-hourly location and maximum wind speed information for all TCs extending back to

8

1851. Additional information has been included in HURDAT2 in more recent years, including

minimum sea level pressure (MSLP) for all Atlantic TCs since 1979 and 34-, 50- and 64-kt wind

radii since 2004. Continental US (CONUS) hurricane landfall intensity information for the 1933

Atlantic hurricane season is derived from HURDAT2 and is obtained from the Atlantic

Oceanographic and Meteorological Laboratory (AOML) website:

https://www.aoml.noaa.gov/hrd/hurdat/UShurrs_detailed.html. Mexican landfalls are calculated

using six-hourly HURDAT2 track data interpolated to three-hourly data as stored in GIS

shapefiles in the International Best Track Archive for Climate Stewardship (IBTrACS) version 4

(Knapp et al. 2010). The maximum sustained wind for each TC when it intersected the Mexican

coastline was taken at its landfalling intensity. Only one landfall — the most intense one — was

counted for each TC, regardless if the TC made landfall in Mexico multiple times (e.g., the

Yucatan Peninsula and then mainland Mexico).

Atmospheric dataset

Atmospheric data are calculated from NOAA-CIRES-DOE 20th Century Reanalysis version 3

(20CRv3) (Slivinski et al. 2019). This dataset is available every 3 hours from 1836–2015. It uses

an Ensemble Kalman Filter (EnKF) methodology with 80 members and the NOAA Global

Forecast System model to generate the needed first guess fields. This EnKF allows the physical

relationships between variables to vary with the synoptic weather situation, for example, some

high pressure systems are associated with heat waves while others are associated with cold

spells. Using the first guess fields, the EnKF will determine how to reconstruct the temperature

and all other variables consistent with the weather situation. For example, a pressure observation

that is higher than the first guess in the middle of a high pressure system would contribute to

reconstructing a warmer temperature in a heatwave but a colder temperature in a cold spell. The

9

only synoptic observations used to derive the reanalysis estimates of the full atmosphere at any particular time are surface and sea level pressure reports from land stations, ships and buoys, as well as TC MSLP values from IBTrACS. Monthly sea ice concentration fields and pentad SST fields are also prescribed as boundary conditions. The SST fields for 1836 to 1980 themselves come from the 8-member Simple Ocean Data Assimilation with sparse input version 3 (SODAsi.3; Giese et al. 2016), while from 1981 to 2015 the SST fields are from the 8-member HadISST2.2 (Rayner et al. 2006). The 20CRv3 ensemble mean and standard deviation output has been regridded from a T254 512×256 Gaussian grid to a regular $1° \times 1°$ grid for ease of use. The 20CRv3 reanalysis is an improvement upon earlier versions of the 20th Century Reanalysis (Compo et al. 2011) due to a higher resolution model forcing the new reanalysis, improved data assimilation methods, an increased ensemble size, and an increased number of surface pressure observations.

Oceanic dataset

In order to be dynamically consistent with the atmospheric fields in 20CRv3, we use skin temperatures (with a land mask) in the 20CRv3 derived from SSTs that are internal to the reanalysis, as discussed in the prior section (e.g., SODAsi.3 and HadISST2.2). These skin temperatures will be referred to as SSTs throughout the remainder of this manuscript. All SST timeseries generated from the combination of these two datasets (e.g., Nino 3.4, Atlantic Main Development Region SSTs, relative SSTs) rank correlate at ~0.9 with similar SST timeseries calculated from NOAA's Extended Reconstructed SST version 5 (ERSSTv5; Huang et al. 2017).

Madden-Julian oscillation index

The Madden-Julian oscillation (MJO) is the dominant mode of tropical convective variability on intraseasonal (~30–70 day) timescales, typically initiating over the Indian Ocean or the western

Pacific Ocean and then propagating eastward along the equator (Madden and Julian 1971, 1972). The MJO has been shown in many studies to impact TC activity through alterations in large-scale conditions such as vertical wind shear, mid-level moisture and vertical motion that can either enhance or suppress TC development and intensification (Camargo et al. 2009, Klotzbach 2014).

One index that has been used frequently to define the location and intensity of the MJO is the Wheeler and Hendon (2004) index (hereafter WH index). This index uses 200-hPa and 850-hPa zonal wind along with outgoing longwave radiation (OLR) observed from polar-orbiting satellites (Liebmann and Smith 1996) which is available since June 1974. To assess the MJO in earlier decades of the 20th century, Oliver and Thompson (2012) developed an MJO index that uses surface pressure observations. This index has now been updated to use ensemble-mean surface pressure fields from 20CRv3 and a multi-variate linear regression of daily surface pressure timeseries covering 1905-2015 at 12 locations in the tropics onto the WH index. This surface pressure-based MJO has been shown to closely resemble the WH index over the period from 1974-2008 (Oliver and Thompson 2012; Oliver 2016) and has also been used in several MJO-TC studies to document the MJO-TC relationship prior to the mid-1970s (Klotzbach and Oliver 2015a, b).

1933 Atlantic Hurricane Season Characteristics

Observed basinwide tropical cyclone activity

11

As was noted in the introduction, the 1933 Atlantic hurricane season was an extremely active one, with 20 named storms, 11 hurricanes, and 6 major hurricanes. Table 2 provides summary statistics for all of the named storms that occurred in 1933, with colloquial names (since Atlantic named storms were not given official names until 1953) for individual storms provided in parentheses when available. Of the six major hurricanes that occurred, two reached Category 5 intensity on the Saffir-Simpson Hurricane Wind Scale — the second consecutive year that multiple Category 5 hurricanes were recorded in the Atlantic basin. The 1932 and 1933 Atlantic hurricane seasons are the only time in the historical record when multiple Category 5 hurricanes have occurred in back-to-back seasons.

Figure 3 displays ACE generated by month during the hurricane season of 1933. The ACE for 2005 and the 1981–2010 average are also provided for comparison. The 1933 Atlantic hurricane season generally followed the canonical seasonal cycle but at a heightened rate of activity with well above-average activity generated from June to October. Both 1933 and 2005 generated more activity in July than in October, while the 1981–2010 average is that more than twice as much ACE is generated in October ($15 * 10^4 \, kt^2$) compared with July ($6 * 10^4 \, kt^2$). In addition to having the overall highest seasonal value of ACE, 1933 was also notable from an ACE perspective for September, generating the second-most ACE ($111 * 10^4 \, kt^2$) for that month in the 1851 to 1933 record, trailing only 1926 ($132 * 10^4 \, kt^2$). Only three Septembers: 1961 ($140 * 10^4 \, kt^2$), 2004 ($155 * 10^4 \, kt^2$) and 2017 ($174 * 10^4 \, kt^2$) have generated more September ACE since 1933.

Observed landfalling hurricane activity

12

Continental United States

The 1933 Atlantic hurricane season was also very active from a landfalling perspective, with

four hurricanes, two of which were at Category 3 (e.g., major hurricane) intensity, making

landfall in the continental US (CONUS) (Fig. 4a), causing ~90 fatalities (Cobb 1991; Barnes

2007; Roth 2010). The average 1900–2019 season had 1.6 CONUS landfalling hurricanes and

0.5 CONUS landfalling major hurricanes, respectively. As noted in the introduction, the two

major hurricanes (Treasure Coast and Cuba-Brownsville) that made landfall in the CONUS did

so just 23 hours apart in early September, causing considerable damage. The Cuba-Brownsville

hurricane also caused 40 fatalities in Texas (Roth 2010), while the Treasure Coast hurricane was

responsible for 2 fatalities in Florida (Barnes 2007). If these hurricanes were to make landfall

today, they would be estimated to cause ~$6 billion USD (Cuba-Brownsville) and ~$2.5 billion

USD (Treasure Coast) using the normalized damage dataset of Weinkle et al. (2018).

The Chesapeake-Potomac hurricane caused the most fatalities (47; Cobb 1991) and caused the

most damage of any hurricane making landfall in the CONUS. The hurricane brought significant

damage from North Carolina to New Jersey, with a seven-foot storm surge observed in Norfolk,

Virginia (Weightman 1933). Figure 5 displays a hindcast of storm tide from the Sea, Lake and

Overland Surges from Hurricanes Model (SLOSH; Jelesnianski et al. 1992) for southeastern

Virginia, highlighting the tremendous inundation that was experienced up the James River.

The Chesapeake-Potomac hurricane was estimated to cost $17,000,000 in 1933 USD using the

base economic damage from Weinkle et al. (2018). Given the tremendous growth in population

and wealth in the mid-Atlantic states along with inflation, the Chesapeake-Potomac hurricane is estimated by Weinkle et al. (2018) to cost between ~$13-$16 billion USD if it were to re-occur today. The base damage estimate of $17,000,000 appears to come from Weightman (1933) who quoted a Weather Bureau Official from Baltimore, Maryland. However, a detailed reading of Weightman (1933) reveals this damage value was only for the state of Maryland. We note that Cobb (1991) estimated the damage of the Chesapeake-Potomac hurricane at $40,000,000 in 1933 USD. We believe that this is a more accurate representation of the observed damage in 1933 from this storm, such that the hurricane would likely cause ~$30-$38 billion USD if it were to re-occur today.

The Florida-Mexico hurricane made landfall near Jupiter, FL as a Category 1 hurricane, then tracked westward across the Gulf of Mexico before making a second landfall in far northern Mexico, also as a Category 1 hurricane. In addition to the four hurricanes that made landfall in the CONUS, the Outer Banks hurricane passed just offshore of Cape Hatteras, but still brought sustained Category 2 winds to the Outer Banks of North Carolina and ~4 feet of storm surge near New Bern (Mitchell 1933b).

Mexico

While the season was very active for CONUS landfalling hurricanes, it had record-setting activity for the Atlantic coast of Mexico (Fig. 4b). Four Atlantic hurricanes made landfall in Mexico in 1933 — the most Atlantic hurricanes making landfall in Mexico in a single year on record. The strongest of these was the Tampico hurricane, which made landfall as a Category 4

14

hurricane with maximum sustained winds estimated at 120 kt on the Yucatan Peninsula before making a second landfall with maximum sustained winds estimated at 95 kt just south of Tampico. This hurricane devastated the Tampico metropolitan area, resulting in ~200 fatalities (Rappaport and Fernandez-Partagas 1995). After making an initial landfall in Jupiter, FL, the Florida-Mexico hurricane continued across the Gulf of Mexico and made a second landfall just south of the Texas border, with over 30 fatalities occurring in northern Mexico, primarily due to flooding (Mitchell 1933a).

Other land areas

In addition to the continental United States and Mexico, several other landmasses were significantly impacted by the landfall of Atlantic hurricanes in 1933. These include the Cuba-Brownsville hurricane's landfall on the northern coast of Cuba as a Category 2 hurricane (Fig. 4a), which caused $11,000,000 in damage in 1933 USD and resulted in ~70 fatalities (Pielke et al. 2003).

Earlier in the season, the Trinidad hurricane made landfall as a Category 1 hurricane in Trinidad, then made another landfall as a Category 1 hurricane in northern Venezuela before turning northwestward and making landfall again in western Cuba as a Category 2 hurricane (Fig. 4a). It then arced to the northwest and then the southwest before making a final landfall near La Pesca, Mexico as a Category 1 hurricane. The system was responsible for 13 fatalities in Trinidad (Mitchell 1933), with a total of 35 fatalities attributed to the hurricane during its lifetime (Rappaport and Fernandez-Partagas 1995).

15

Near the end of the season, the Cuba-Bahamas hurricane formed in the western Caribbean and made landfall in western Cuba as a Category 2 hurricane (Fig. 4a). It then turned towards the northeast, passing south of the Florida Keys and tracking over the northwest Bahamas as a Category 3 hurricane. It became a powerful post-tropical storm over the North Atlantic, causing nine fatalities and resulting in at least $1 million in damage in Nova Scotia when it tracked just southeast of the province (Environment Canada, 1933).

Large-scale atmosphere-ocean conditions

In order to examine the favorability of large-scale atmosphere-ocean conditions during the peak of the 1933 Atlantic hurricane season (August-October), we examine anomalies of MSLP, zonal wind shear (defined as the difference in the U component of the wind between 200 hPa and 850 hPa), and SST averaged over the Main Development Region (MDR), which we define to be 10-20°N, 85-20°W. All of these quantities have been shown in prior studies (e.g., Saunders et al. 2017 and references therein) to explain a significant amount of the variance in observed Atlantic hurricane activity. Lower MSLP, reduced vertical wind shear, and higher SSTs are favorable for an active Atlantic hurricane season. In addition to conditions in the Atlantic MDR, we also examine ENSO conditions using SST in the Niño 3.4 region (5°S–5°N, 170–120°W) (Barnston et al. 1997) and relative SST, which is defined to be SST in the tropical Atlantic (10–25°N, 80–20°W) minus average SST across the greater tropics (30°S–30°N, 0–360°) (Vecchi and Sobel 2008). El Niño conditions are unfavorable for Atlantic hurricane development and intensification due to both increases in vertical wind shear (e.g., Gray 1984) and warmer upper-level temperatures that stabilize the atmosphere (Tang and Neelin 2004). Positive values of relative SST imply that the Atlantic is warm relative to the rest of the tropics. This is associated

16

with conditions more conducive to Atlantic hurricane formation: increased upward motion, increased low-level vorticity, and reduced vertical wind shear (Vecchi and Sobel 2008). Anomalies are calculated relative to the 1901–1930 base period, which would have been the 30-year base period in 1933 given NOAA's current practices (e.g., 30-year base periods updated every ten years). Our examination of 1933 is complemented by a correlation and a rank analysis of more than a century of variability in these quantities associated with Atlantic hurricane activity. These analyses begin in 1878, as this is when the US Signal Service Corps began to track hurricanes in a systematic fashion (Vecchi and Knutson 2011; Saunders et al. 2017).

Figure 6a–d displays 1933 August–October-averaged anomalies of SLP, zonal wind shear, SST, and 500 geopotential height across the Atlantic and, in the case of SST, including the eastern-central Pacific. As would be expected given the extremely active season that occurred, large-scale conditions were favorable for an active Atlantic hurricane season with anomalously low MSLP, anomalously weak zonal wind shear, and warmer-than-normal SSTs prevailing across the MDR. Weak-to-moderate La Niña conditions prevailed across the tropical Pacific. Anomalously high heights at 500 hPa predominated over the subtropical western Atlantic, creating mid-level steering flow that inhibited recurvature and drove hurricanes towards the US, Mexico, Central America, and through the Caribbean.

Since 2005 was also an extremely active season and has been compared to 1933 in this manuscript, we also examine large-scale conditions during August–October of that year (Figure 6e-f). For these plots, we calculate anomalies relative to a 1971–2000 base period, which would have been the 30-year base period utilized by NOAA at the time. Similar to 1933, the 2005

17

Atlantic hurricane season featured anomalously low MSLP, warmer-than-normal SSTs and weaker than normal zonal wind shear across the MDR. Unlike 1933, ENSO was neutral during the peak of the 2005 Atlantic hurricane season, with an August-October-averaged Oceanic Nino Index of -0.1°C. The Oceanic Nino Index is defined to be a three-month running mean of SST anomalies in the Nino 3.4 region (5°S–5°N, 170°W–120°W) using centered 30-year base periods. Geopotential heights at 500 hPa tended to be above average in the western Atlantic, helping to steer storms towards the US coast as well as the Caribbean and Central America.

In order to quantify the favorability of 1933, Table 3 provides standardized anomalies relative to the 1901–1930 base period and also 1933's rank relative to all Atlantic hurricane seasons from 1878–1933 for SLP, zonal wind shear, MDR SST, Niño 3.4 and relative SST. For reference, the rank of 1933 relative to all Atlantic hurricane seasons from 1878–2015 (when the 20CRv3 currently ends), are also provided. The ranks listed in parentheses for the atmospheric fields are based off of the 80 ensemble members comprising 20CRv3. These values represent the 95% confidence interval of the ranks (e.g., 76 of the 80 ensemble members have ranks between those two values). We do not include ranks for the SST parameters, as these are derived from an 8-member ensemble. To highlight the relative importance of the dominant large-scale atmospheric conditions in years excluding 1933, we also provide rank correlations (to diminish the impact of strong outlier events) between each parameter and Atlantic ACE over 1878–1932, 1934–1965, and 1966–2015 (e.g., the satellite era; Vecchi and Knutson 2011). Correlations significant at the 5% level using a two-tailed Student's t-test are highlighted in bold.

18

Sea level pressure, zonal wind shear, MDR SST, Niño 3.4 and relative SST were all favorable for an active season in 1933. All ranks discussed in the following section are relative to the 1878–1933 base period. While zonal wind shear ranked 9th most favorable when averaged across the entire MDR, these anomalies were of an even larger magnitude when considering only the western Atlantic. MDR SST was also the 9th most favorable, although we note that there have been many years since 1933 with warmer MDR SSTs, due primarily to the long-term anthropogenic warming trend (Knutson et al. 2019). However, as was noted in Vecchi et al. (2008) and seen in Table 3, Atlantic TC activity correlates better with relative SST than it does with MDR SST, which is likely why there is no long-term trend in Atlantic hurricane activity when adjusting for potentially missed hurricanes prior to the satellite era (Vecchi and Knutson 2008). Relative SST in 1933 was the fourth highest on record, indicating that in addition to favorable shear and SST conditions, vertical motion, and low-level vorticity were also likely enhanced over the Atlantic in 1933, providing conditions that were extremely conducive for an active season.

It is important to recognize that there is more uncertainty in the large-scale conditions of 1933 compared with later in the record. Figure 7 displays MDR-averaged zonal vertical wind shear based on the ensemble mean from 1836–2015 along with the 95% confidence interval assuming that the errors are normally distributed (i.e., ensemble mean ± 1.96*ensemble standard deviation). In addition to the increased uncertainty early in the record, we note that 20CRv3 also identifies extremely low vertical wind shear in the late 1800s — a time period which had several extremely active Atlantic hurricane seasons, especially 1878, 1886, 1887, and 1893. All four of these seasons had observed ACE over 160, which are likely considerable under-estimates given

19

the sparse available observational data in the late 19th century (Landsea et al. 2004). However, given the uncertainty in the ensemble members, we cannot conclusively assert that the vertical wind shear in the late 19th century was less than what has been observed in more recent active multi-decadal hurricane periods (Goldenberg et al. 2001).

Note that the magnitude of all correlations with ACE drops during 1934–1965 from either the 1878–1932 or the 1966–2015 period (Table 3). A similar dropout in parameter skill was noted in Saunders et al. (2017). While it is likely somewhat driven by data paucity issues during World War II, it may also reflect low interannual variability during this time period (e.g., Torrence and Compo 1998; Torrence and Webster 1999). Caron et al. (2015) noted that certain Atlantic predictors showed more skill in specific phases of the Atlantic multidecadal oscillation (AMO), so this may have also played a role in the 1933–1965 correlation dropout. All of the large-scale parameters examined above have significant correlations with Atlantic ACE during both the 1878–1932 and 1965–2015 periods.

Subseasonal variability

In addition to the seasonal factors, subseasonal variability also likely played a role in observed Atlantic hurricane activity in 1933. While the MJO amplitude was not extremely high during most of the 1933 Atlantic hurricane season, there were several periods where it likely affected TC formation and intensification (Fig. 8a,b). The Atlantic was extremely active from mid-August through early September (Fig. 8c), when the MJO was in phases 1–3 (e.g., enhanced

20

convection over Africa and the Indian Ocean) and generally had an amplitude exceeding one (Fig. 8d). An MJO index exceeding one has been used in several studies to represent periods when MJO activity is enhanced (e.g., Klotzbach 2014; Klotzbach and Oliver 2015a, b; Wang and Moon 2017). MJO phases 1–3 tend to be associated with active Atlantic hurricane periods, due to anomalous reductions in vertical wind shear and increases in mid-level moisture (Camargo et al. 2009; Ventrice et al. 2011; Klotzbach 2014). The latter part of the Atlantic TC season (e.g., after ~10 October) was relatively quiet, likely associated with phases of the MJO unfavorable to TC activity (e.g., Phases 5–7 where convection is favored over the Maritime Continent and Western Pacific) from mid-to-late October (Fig. 8b).

Klotzbach and Oliver (2015a) showed, based on data from 1905–2011, that MJO phases 1 and 2 tend to favor the most Atlantic TC activity, and this relationship held true in 1933. During the 1933 Atlantic hurricane season, 36% of all days where the MJO amplitude was greater than one occurred in phases 1 and 2. These days generated 60% of all Atlantic ACE that was generated when the MJO amplitude was greater than one. MJO phases 1 and 2 generated ACE at 167% (e.g., 60% of Atlantic ACE / 36% of days) of the average daily ACE generation rate when the MJO was greater than one during the 1933 Atlantic hurricane season.

4.   How well would the 1933 Atlantic hurricane season have been anticipated by current statistical models?

21

In this section, we examine how the current early June and early August statistical model used by Colorado State University (Klotzbach et al. 2020a; 2020b) would have anticipated the peak of the 1933 Atlantic hurricane season given observed large-scale conditions. An in-depth discussion of how the predictors in these statistical models likely impacts Atlantic hurricanes is given in Klotzbach et al. (2020a; 2020b).

June statistical forecast model

As was done in Table 3, Table 4 summarizes each parameter, provides the value of its standardized anomaly relative to the 1901–1930 base period, and ranks its 1933 value compared with all Atlantic hurricane seasons from 1878–1933 as well as during the period of 1878–2015. 95% confidence intervals are also provided for ranks of atmospheric parameters. We also include rank correlations between each predictor and Atlantic ACE during the periods from 1878–1932, 1934–1965, and 1966–2015. Correlations significant at the 5% level using a two-tailed Student t-test are highlighted in bold. All four parameters are favorable for Atlantic hurricane activity, with three of the four predictors greater than one standard deviation favorable. Similar to the case for the diagnostic parameters during August–October, we note that all four predictors have very low (and insignificant) correlations with Atlantic ACE during the 1934–1965 period. We also find that the correlation between Atlantic ACE and the zonal wind predictor in the tropical Pacific is insignificant from 1878–1932, but this region likely had very few observations during this earlier time period which may account for the lack of a relationship.

22

We next examine how well this four-predictor model would forecast Atlantic hurricane activity in 1933 if it had been developed on data from 1878–1932. We use a linear regression of the four predictors against Atlantic ACE and display ACE ranks, with lower ranks meaning less ACE. The resulting predictive equation explains ~40% of the variance (r_{rank} = 0.62) in ACE from 1878–1932 (Fig. 9). This same model would have predicted that Atlantic ACE in 1933 would be the 7th highest on record (from 1878–1933), which would have equated to an ACE of ~165 * 10^4 kt^2. Consequently, the current early June statistical model from CSU, while not calling for the most active season on record, would have called for an "extremely active" Atlantic hurricane season in 1933 using NOAA's current hurricane season definition (ACE: >152.5 *10^4 kt^2) (https://www.cpc.ncep.noaa.gov/products/outlooks/Background.html).

August statistical forecast model

We now evaluate the skill of the August statistical forecast model at predicting post-31 July ACE in 1933. Table 5 summarizes the predictors, their ranks relative to all Atlantic hurricane seasons from 1878–1933 and 1878–2015 as well as their rank correlations with ACE during 1878–1933, 1934–1965, and 1966–2015. 95% confidence intervals are also provided for ranks of atmospheric parameters. Each of the three predictors are at least one standard deviation favorable for Atlantic hurricane activity and show significant correlations with ACE during 1878–1933 and 1966–2015, with insignificant correlations during 1934–1965.

We next examine how well this three-predictor model would forecast Atlantic hurricane activity in 1933 if it had been developed on data from 1878–1932. We use a linear regression of the three predictors against Atlantic ACE and display ACE ranks, with lower ranks meaning less ACE. The resulting predictive equation explains ~40% of the variance ($r_{rank} = 0.62$) in post-31 July ACE from 1878–1932 (Fig. 10). This same model would have predicted that post-31 July Atlantic ACE in 1933 would be the 4th highest on record (from 1878–1933), which would have equated to a post-31 July ACE of ~179 * 10^4 kt^2. Since observed activity through 31 July in 1933 was 49 * 10^4 kt^2, the full seasonal forecast in early August would have been for an ACE of 228 * 10^4 kt^2.

In addition to CSU's current early August predictors, we also note that 1933 had more named storm days (9.75 days) prior to 1 August in the tropical Atlantic (south of 23.5°N, east of 75°W; Klotzbach 2007) than any other year on record. Early season activity in the deep tropics, while not a necessary condition for an active season, typically heralds a very active season (Klotzbach 2007). Early season activity in the deep tropics is typically restricted due to a TC-unfavorable thermodynamic environment (e.g., dry air, cool SSTs; DeMaria et al. 2001), and consequently, early season TC activity in the deep tropics is associated with a TC-favorable thermodynamic environment that likely then persists for the remainder of the season.

In summary, both the current June and August statistical models from CSU show skill at predicting seasonal Atlantic ACE from 1878–1932 and both anticipate a very active Atlantic hurricane season in 1933. The very active TC activity in the tropical Atlantic prior to 1 August also presaged the extreme levels of hurricane activity that were experienced.

24

5.   Summary and Implications

The 1933 Atlantic hurricane season was one of the most active on record, with 20 named storms, 11 hurricanes, and 6 major hurricanes occurring. The season currently holds the record for the most Atlantic ACE generated in a single year since 1851 (Landsea et al. 2014) and was also extremely active for landfalls, with four hurricanes making landfall in the continental US. Two of these hurricanes did so as Category 3 hurricanes just 23 hours apart in Florida and Texas, respectively. Eight hurricanes tracked through the Caribbean, and four Atlantic hurricanes made landfall in Mexico — both records in the Atlantic hurricane database (Landsea and Franklin 2013).

As would be expected given how active the season was, large-scale conditions were quite conducive for hurricane activity, with anomalously warm SSTs, anomalously weak vertical wind shear, and anomalously low MSLP predominating over the MDR. In addition, 500 hPa geopotential height fields featured stronger-than-normal ridging over most of the western Atlantic, inhibiting TC recurvature and driving storms farther west towards the Caribbean, Central America and the United States.

Both the current early June and early August CSU statistical models for Atlantic ACE called for a very active season in 1933. These models also were shown to have skill at predicting the 1878–1932 Atlantic hurricane seasons, explaining ~40% of the variance in ACE at both lead times.

25

While many consider that 2005 was the most active Atlantic hurricane season on record, we note that 1933 had nearly as much activity as 2005 for several parameters (Table 1) and more activity for ACE, despite a lack of aircraft reconnaissance and satellite observations. While there is no way to know how many storms were missed in 1933, the season likely had more activity than what is currently recorded in HURDAT2 (Vecchi and Knutson 2008; Landsea et al. 2014). A more thorough analysis of missed storms including an analysis of potential underestimated aggregate storm statistics such as ACE would be a welcome addition to the historical record. The season was also quite destructive, highlighting the dangers of extremely favorable large-scale conditions combined with steering patterns driving hurricanes towards landmasses, similar to what was seen in both 2005 and more recently in 2017 (Klotzbach et al. 2018b). Given the large growth in population and wealth in coastal areas (Klotzbach et al. 2018a; Weinkle et al. 2019), and any further enhancements to the atmospheric and oceanic environments via climate change (Knutson et al. 2019), Atlantic hurricane seasons with activity on par with years like 1933, 2005, and 2017 are likely to cause even more physical damage when they occur in the future.

26

Data Availability Statement

All of the data used in this study is publicly available at the following URLs:

Continental US hurricane landfalls:

https://www.aoml.noaa.gov/hrd/hurdat/UShurrs_detailed.html

HURDAT2:

https://www.aoml.noaa.gov/hrd/hurdat/hurdat2.html

IBTrACS v4:

https://www.ncdc.noaa.gov/ibtracs/

NOAA-CIRES-DOE 20th Century Reanalysis version 3 ensemble member fields:

https://portal.nersc.gov

NOAA-CIRES-DOE 20th Century Reanalysis version 3 ensemble mean fields:

https://psl.noaa.gov

Oceanic Nino Index:

https://origin.cpc.ncep.noaa.gov/products/analysis_monitoring/ensostuff/ONI_v5.php

Reconstructed MJO index:

http://passage.phys.ocean.dal.ca/~olivere/data/mjoindex_IHR_20CRV3.dat

28

References

Barnes, J., 2007: Florida's Hurricane History. University of North Carolina Press, 424 pp.

Barnston, A. G., M. Chelliah, and S. B. Goldenberg, 1997: Documentation of a highly ENSO-related SST region in the equatorial Pacific: Research note. *Atmosphere-Ocean,* **35**, 367-383, https://doi.org/10.1080/07055900.1997.9649597.

Bell, G. D., and Coauthors, 2000: Climate assessment for 1999. *Bull. Amer. Meteor. Soc.,* **81,** 1328, https://doi.org/10.1175/1520-0477(2000)81[s1:CAF]2.0.CO;2.

Beven, J. L., L. A. Avila, E. S. Blake, D. P. Brown, J. L. Franklin, R. D. Knabb, R. J. Pasch, J. R. Rhome, and S. R. Stewart, 2008: Atlantic hurricane season of 2005. *Mon. Wea. Rev.,* **136,** 1108-1173, https://doi.org/10.1175/2007MWR2074.1.

Camargo, S. J., M. C. Wheeler, and A. H. Sobel, 2009: Diagnosis of the MJO modulation of tropical cyclogenesis using an empirical index. *J. Atmos. Sci.,* **66,** 3061–3074, https://doi.org/10.1175/2009JAS3101.1.

Caron, L.-P., M. Boudreault, and C. L. Bruyere, 2015: Changes in large-scale controls of Atlantic tropical cyclone activity with the phases of the Atlantic multidecadal oscillation. *Climate Dynamics,* **44,** 1801-1821, https://doi.org/10.1007/s00382-014-2186-5.

Cobb, H. D., 1991: The Chesapeake-Potomac hurricane of 1933. *Weatherwise,* **44,** 24-29, https://doi.org/10.1080/00431672.1991.9929376

Compo, G. P., and Co-authors, 2011: The Twentieth Century Reanalysis Project. *Quart. J. Roy. Meteorol. Soc.,* **137,** 1-28, http://dx.doi.org/10.1002/qj.776.

DeMaria, M., J. A. Knaff, and B. H. Connell, 2001: A tropical cyclone genesis parameter for the tropical Atlantic. *Wea. Forecasting*, **16**, 219–233, https://doi.org/10.1175/1520-0434(2001)016<0219:ATCGPF>2.0.CO;2.

Environment Canada, 1933: Detailed Storm Impacts - 1933-18 (Report). Environment Canada. 2009-11-18. Retrieved 2013-10-01.

Giese, B. S., H. F. Seidel, H. F., G. P. Compo, and P. D. Sardeshmukh, 2016: An ensemble of ocean reanalyses for 1815–2013 with sparse observational input. *J. Geophys. Res. Oceans*, **121,** 6891– 6910, https://doi.org/10.1002/2016JC012079.

Gray, W. M., 1984: Atlantic seasonal hurricane frequency. Part I: El Niño and 30 mb quasi-biennial oscillation influences. *Mon. Wea. Rev.,* **112,** 1649–1668, https://doi.org/10.1175/1520-0493(1984)112%3C1649:ASHFPI%3E2.0.CO;2.

Huang, B., P. W. Thorne, V. F. Banzon, T. Boyer, G. Chepurin, J. H. Lawrimore, M. J. Menne, T. M. Smith, R. S. Vose, and H. Zhang, 2017: Extended Reconstructed Sea Surface Temperature, Version 5 (ERSSTv5): Upgrades, validations, and intercomparisons. *J. Climate,* **30**, 8179–8205, https://doi.org/10.1175/JCLI-D-16-0836.1.

Insurance Information Institute, 2019: Florida's assignment of benefits crisis. 31 pp, https://www.iii.org/sites/default/files/docs/pdf/aobfl_wp_031319.pdf.

Jelesnianski, C. P., J. Chen, and W. A. Shaffer, 1992: SLOSH: Sea, lake, and overland surges from hurricanes. NOAA Tech. Report NWS 48, 71 pp. [Available from NOAA/AOML Library, 4301 Rickenbacker Cswy., Miami, FL 33149.].

Klotzbach, P. J., 2007: Revised prediction of seasonal Atlantic basin tropical cyclone activity from 1 August. *Wea. Forecasting*, **22**, 937–949, https://doi.org/10.1175/WAF1045.1.

Klotzbach, P. J., 2014: The Madden–Julian oscillation's impacts on worldwide tropical cyclone activity. *J. Climate,* **27,** 2317–2330, https://doi.org/10.1175/JCLI-D-13-00483.1.

___, M. M. Bell, and J. Jones, 2020a: Extended range forecast of Atlantic seasonal hurricane activity and landfall strike probability for 2020. Dept. of Atmospheric Science Report, Colorado State University, Fort Collins, CO, 36 pp, https://tropical.colostate.edu/Forecast/2020-06.pdf.

___, M. M. Bell, and J. Jones, 2020b: Forecast of Atlantic seasonal hurricane activity and landfall strike probability for 2020. Dept. of Atmospheric Science Report, Colorado State University, Fort Collins, CO, 31 pp, https://tropical.colostate.edu/Forecast/2020-08.pdf.

___, and E. C. J. Oliver, 2015a: Modulation of Atlantic basin tropical cyclone activity by the Madden-Julian Oscillation (MJO) from 1905-2011, *J. Climate,* **28,** 204-217, https://doi.org/10.1175/JCLI-D-14-00509.1.

___, and E. C. J. Oliver, 2015b: Variations in global tropical cyclone activity and the Madden-Julian Oscillation since the midtwentieth century, *Geophys. Res. Lett,* **42,** 4199-4207, https://doi.org/10.1002/2015GL063966.

___, S. G. Bowen, R. Pielke Jr., and M. M. Bell, 2018a: Continental United States landfall frequency and associated damage: Observations and future risks. *Bull. Amer. Meteor. Soc.,* **99,** 1359-1376, https://doi.org/10.1175/BAMS-D-17-0184.1.

___, P. J., C. J. Schreck III, J. M. Collins, M. M. Bell, E. S. Blake, and D. R. Roache, 2018: The extremely active 2017 North Atlantic hurricane season. *Mon. Wea. Rev.,* **146,** 3425-3443, https://doi.org/10.1175/MWR-D-18-0078.1.

Knapp, K.R., M.C. Kruk, D.H. Levinson, H.J. Diamond, and C.J. Neumann, 2010: The International Best Track Archive for Climate Stewardship (IBTrACS). *Bull. Amer. Meteor. Soc.,* **91**, 363–376, https://doi.org/10.1175/2009BAMS2755.1.

Knutson, T., S. J. Camargo, J. C. Chan, K. Emanuel, C. Ho, J. Kossin, M. Mohapatra, M. Satoh, M. Sugi, K. Walsh, and L. Wu, 2019: Tropical cyclones and climate change assessment: Part I: Detection and attribution. *Bull. Amer. Meteor. Soc.,* **100**, 1987–2007, https://doi.org/10.1175/BAMS-D-18-0189.1

Landsea, C. W., C. Anderson, N. Charles, G. Clark, J. Dunion, J. Partagas, P. Hungerford, C. Neumann and M. Zimmer, 2004: The Atlantic hurricane database re-analysis project: Documentation for the 1851-1910 alterations and additions to the HURDAT database. hurricanes and Typhoons: Past, Present and Future, R. J. Murnane and K.-B. Liu, Eds., Columbia University Press, 177-221, https://doi.org/10.1029/2005EO160008

Landsea, C. W., and J. L. Franklin, 2013: Atlantic hurricane database uncertainty and presentation of a new database format. *Mon. Wea. Rev.,* **141,** 3576–3592, https://doi.org/10.1175/MWR-D-12-00254.1.

___, A. Hagen, W. Bredemeyer, C. Carrasco, D. A. Glenn, A. Santiago, D. Strahan-Sakoskie, and M. Dickinson, 2014: A reanalysis of the 1931-43 Atlantic hurricane database. *J. Climate,* **27,** 6093-6118, https://doi.org/10.1175/JCLI-D-13-00503.1.

___, G. A. Vecchi, L. Bengtsson, and T. R. Knutson, 2010: Impact of duration thresholds on

Atlantic tropical cyclone counts. *J. Climate,* **23,** 2508-2519,

https://doi.org/10.1175/2009JCLI3034.1.

Liebmann, B., and C. A. Smith, 1996: Description of a complete (interpolated) outgoing

longwave radiation dataset. *Bull. Amer. Meteor. Soc*, **77,** 1275–1277,

https://www.jstor.org/stable/26233278

Madden, R. A., and P. R. Julian, 1971: Detection of a 40-50 day oscillation in the zonal wind in

the tropical Pacific. *J. Atmos. Sci.,* **28,** 702–708, https://doi.org/10.1175/1520-

0469(1971)028%3C0702:DOADOI%3E2.0.CO;2.

___, and ___, 1972: Description of global-scale circulation cells in the tropics with a 40-50 day

period. *J. Atmos. Sci.,* **29,** 1109–1123, https://doi.org/10.1175/1520-

0469(1972)029%3C1109:DOGSCC%3E2.0.CO;2.

Mitchell, C. L., 1933a: Tropical disturbances of July 1933. *Mon. Wea. Rev.,* **61,** 200-201,

https://doi.org/10.1175/1520-0493(1933)61%3C200b:TDOJ%3E2.0.CO;2

___, 1933b: Tropical disturbances of September 1933. *Mon. Wea. Rev.,* **61,** 274-276,

https://doi.org/10.1175/1520-0493(1933)61%3C274:TDOS%3E2.0.CO;2

Oliver, E. C. J., 2016: Blind use of reanalysis data: Apparent trends in Madden-Julian Oscillation

activity driven by observational changes. *International J. of Climatology,* **36,** 3458-3468,

https://doi.org/10.1002/joc.4568.

Oliver, E. C. J., and K. R. Thompson, 2012: A reconstruction of Madden–Julian Oscillation variability from 1905 to 2008. *J. Climate,* **25,** 1996–2019, https://doi.org/10.1175/JCLI-D-11-00154.1.

Pielke, R. A., J. Rubiera, C. W. Landsea, M. L. Fernandez, and R. Klein, 2003: hurricane vulnerability in Latin America and the Caribbean: Normalized damage and loss potentials. *Natural Hazards Review,* **4,** 101-114, https://doi.org/10.1061/(ASCE)1527-6988(2003)4:3(101).

Rappaport, E. N., and J. Fernandez-Partagas, 1995: The deadliest Atlantic tropical cyclones: 1492-1994. *NOAA Tech. Memo 47,* 42 pp., https://www.nhc.noaa.gov/pdf/NWS-NHC-1995-47.pdf

Rayner, N.A., P. Brohan, D. E. Parker, C. K. Folland, J. J. Kennedy, M. Vanicek, T .J. Ansell, and S.F. Tett, 2006: Improved analyses of changes and uncertainties in sea surface temperature measured in situ since the mid-nineteenth century: The HadSST2 Dataset. *J. Climate,* **19**, 446–469, https://doi.org/10.1175/JCLI3637.1

Roth, D., 2010: Texas hurricane history. *Hydrometeorological Prediction Center Report,* 83 pp. https://www.wpc.ncep.noaa.gov/research/txhur.pdf

Saunders, M. A., P. J. Klotzbach, and A. S. R. Lea, 2017: Replicating annual North Atlantic hurricane activity 1878-2012 from environmental variables. *J. Geophys. Res.-Atmospheres,* **122,** 6284-6297, https://doi.org/10.1002/2017JD026492.

Slivinski, L. C., and Co-authors, 2019: Towards a more reliable historical reanalysis: Improvements for version 3 of the Twentieth Century Reanalysis system. *Quart. J. Roy. Meteorol. Soc.,* **145,** 2876– 2908, https://doi.org/10.1002/qj.3598.

34

Tang, B. H., and J. D. Neelin, 2004: ENSO influence on Atlantic hurricanes via tropospheric warming. *Geophys. Res. Lett.,* **31,** L24204, https://doi.org/10.1029/2004GL021072.

Torrence, C., and G. P. Compo, 1998: A practical guide to wavelet analysis. *Bull. Amer. Meteor. Soc.,* **79,** 61-78, https://doi.org/10.1175/1520-0477(1998)079%3C0061:APGTWA%3E2.0.CO;2.

___, and P. J. Webster, 1999: Interdecadal changes in the ENSO-monsoon system. *J. Climate,* **12,** 2679-2690, https://doi.org/10.1175/1520-0442(1999)012%3C2679:ICITEM%3E2.0.CO;2.

Vecchi, G. A., and T. R. Knutson, 2008: On estimates of historical North Atlantic tropical cyclone activity. *J. Climate*, **21,** 3580–3600, https://doi.org/10.1175/2008JCLI2178.1.

___, K. L. Swanson, and B. J. Soden, 2008: Wither hurricane activity? *Science,* **322,** 687–689, https://doi.org/10.1126/science.1164396.

___, and T. R. Knutson, 2011: Estimating annual numbers of Atlantic hurricanes missing from the HURDAT database (1878–1965) using ship track density. *J. Climate,* **24,** 1736–1746, https://doi.org/10.1175/2010JCLI3810.1.

Ventrice, M. J., C. D. Thorncroft, and P. E. Roundy, 2011: The Madden Julian Oscillation's influence on African easterly waves and downstream tropical cyclogenesis. *Mon. Wea. Rev.*, 139, 2704-2722, https://doi.org/10.1175/MWR-D-10-05028.1.

Wang, B., and J.-Y. Moon, 2017: An anomalous genesis potential index for MJO modulation of tropical cyclones. *J. Climate,* **30,** 4021-4035, https://doi.org/10.1175/JCLI-D-16-0749.1.

Weightman, R. H., 1933: Tropical disturbances of August 1933. *Mon. Wea. Rev.,* **61,** 233-234, https://doi.org/10.1175/1520-0493(1933)61%3C233b:TDOA%3E2.0.CO;2.

35

Weinkle, J., C. W. Landsea, D. Collins, R. Masulin, R. P. Crompton, P. J. Klotzbach, and R.

Pielke Jr., 2018: Normalized hurricane damage in the continental United States: 1900-2017.

Nature Sustainability, 1, 803-813, https://doi.org/10.1038/s41893-018-0165-2.

Wheeler, M. C., and H. H. Hendon, 2004: An all-season real-time multivariate MJO index:

Development of an index for monitoring and prediction. *Mon. Wea. Rev.,* **132,** 1917–1932,

https://doi.org/10.1175/1520-0493(2004)132%3C1917:AARMMI%3E2.0.CO;2.

Sidebar: How would the insurance industry cope with a repeat of the 1933 Atlantic hurricane season?

Active years for natural catastrophes in the United States are not out of the ordinary. Various governmental agencies and private sector groups are well trained and positioned to ensure quick response in the aftermath of a major event. But what happens when major events occur within quick succession? This is a question that poses numerous challenges, especially for the insurance industry. A repeat of the 1933 Atlantic hurricane season today would create many strategic difficulties for insurers being able to activate enough claims assessors and ensure a quick and smooth claim process for those hardest-hit.

The historic Atlantic hurricane season in 2017 — combined with major wildfires in the state of California — provided a recent example of the challenges faced for insurers. Following the landfalls of Harvey, Irma, and Maria, these events left the insurance industry stretched thin as the damage footprint in each instance was considerable. These storms were then followed by major wildfire ignitions across northern and southern California during October and December, respectively. All of this led to prolonged claims filings and approvals and also resulted in many affected homeowners and business owners turning to third-party groups to initiate and make repair decisions individually. In those cases, the third-party groups would bill the insurance company, and sometimes include unnecessary or higher-cost repairs that would not have been approved had a standard insurance assessor conducted an analysis. This process, known as an "assignment of benefits" (AOB), is often susceptible to fraudulent practices and high-cost lawsuits in the aftermath of large-scale disasters (Insurance Information Institute 2019). When AOB is particularly egregious and widespread, this can result in higher premiums for consumers

37

as a result of heightened claims payouts and litigation costs. It even resulted in the state of Florida passing legislation to reform the practice in 2019. Another major issue for insurers after multiple large events is demand surge. This is defined as the increased cost of repair and/or replacement associated with a limited supply of labor and materials in the aftermath of multiple large scale events. If multiple major hurricane landfalls were to occur in such rapid succession as they did in 1933, it would undoubtedly lead to equally prolonged claim filings and approval challenges as seen in 2017.

While the reinsurance industry had more than $625 billion USD in available capital at the end of 2019 — ensuring the health of the industry and its ability to withstand multiple, quick succession events — the biggest challenge will remain having enough resources to observe and process the damage in the immediate aftermath. While 2017 provided numerous learning opportunities, a repeat of the 1933 Atlantic hurricane season would inevitably prove difficult.

Table 1: Observed Atlantic TC statistics in 1933, 2005, and the 1981–2010 average. Also included in parentheses in the 1933 and 2005 columns are ranks for each TC statistic (since 1851 when HURDAT2 begins). A 'T' in parentheses denotes a tie with other seasons.

TC Statistic	1933	2005	1981–2010 Average
Named Storms	20 (2)	28 (1)	12.1
Named Storm Days	125.25 (2)	126.25 (1)	59.4
Hurricanes	11 (T-4)	15 (1)	6.4
Hurricane Days	57.00 (4)	49.75 (8)	24.2
Major Hurricanes	6 (T-2)	7 (1)	2.7
Major Hurricane Days	21.75 (5)	17.50 (7)	6.2
Accumulated Cyclone Energy	259 (1)	245 (2)	106

Table 2: Individual storm statistics for all named storms of the 1933 Atlantic hurricane season.
Also listed are the maximum category that the storm reached on the Saffir-Simpson Hurricane
Wind Scale, with systems not reaching hurricane strength being noted as tropical storms (TS).

Storm Number (Colloquial Name)	Maximum Lifetime Intensity (kt)	Named Storm Days	Hurricane Days	Major Hurricane Days	ACE	Maximum Saffir-Simpson category
1	45	4.75	---	---	3.1	TS
2 (Trinidad)	95	12.75	9.75	---	29.1	2
3	45	5.00	---	---	3.0	TS
4	50	2.00	---	---	1.5	TS
5 (Florida-Mexico)	80	12.00	6.00	0.00	17.9	1
6 (Chesapeake-Potomac)	120	11.00	7.25	4.75	33.7	4
7	40	4.00	---	---	2.0	TS
8 (Cuba-Brownsville)	140	11.00	7.75	6.25	40.2	5
9	55	4.75	---	---	3.4	TS
10	35	1.00	---	---	0.5	TS
11 (Treasure Coast)	120	7.00	4.00	2.00	17.9	4
12 (Outer Banks)	120	10.25	8.50	4.75	35.7	4
13	95	5.00	1.25	---	6.7	2

40

14 (Tampico)	140	7.75	5.25	2.50	25.9	5
15	65	2.75	0.75	---	3.8	1
16	40	2.00	---	---	1.1	TS
17 (Cuba-Bahamas)	110	6.75	5.00	1.50	17.9	3
18	80	11.50	1.50	---	11.2	1
19	60	2.50	---	---	2.9	TS
20	50	1.50	---	---	1.1	TS

41

Table 3: August-October MDR-averaged SLP, zonal wind shear (ZWS), and SST standardized anomalies relative to a 1901–1930 base period. Also displayed are Nino 3.4 and relative SST anomalies. The sign of each parameter associated with more active Atlantic hurricane seasons is noted in parentheses. Ranks of each parameter in 1933 compared with all seasons from 1878–1933 as well as from 1878–2015 are also included. Ranks in parentheses for the atmospheric fields represent the 95% confidence intervals for each rank. Signs of ranks have been reversed for parameters that correlate negatively with ACE (e.g., MDR SLP, zonal wind shear) for easy comparison. Also provided are linear correlations between each parameter and ACE from 1878–1932, 1934–1965 and 1966–2015. Correlations significant at the 5% level are highlighted in bold.

Statistic	SLP (-)	ZWS (-)	SST (+)	Niño 3.4 (-)	Relative SST (+)
1933 Standardized Value	-0.9	-1.7	+1.7	-1.5	+1.9
1933 Rank (1878–1933)	20 (8–38)	9 (4–18)	9	4	4
1933 Rank (1878–2015)	25 (10–48)	10 (4–23)	41	5	9
1878–1932 Rank Correlation w/ ACE	**-0.62**	**-0.69**	**0.46**	**-0.42**	**0.56**
1934–1965 Rank Correlation w/ ACE	-0.17	**-0.41**	-0.03	-0.19	-0.04
1966–2015 Rank Correlation w/ ACE	**-0.63**	**-0.77**	**0.57**	**-0.40**	**0.70**

42

Table 4: As in Table 3 but for the current early June statistical hurricane forecast model (Klotzbach et al. 2020a). The four predictors are April-May-averaged SST "North Atlantic" SST averaged over 20–60°N, 40–15°W, May SLP "Subtropical Atlantic" SLP averaged over 20–40°N, 60–10°W, May 10 meter zonal wind "Tropical Pacific U" averaged over 5°S-5°N, 180°-130°W and April-May-averaged SST "Coral Sea SST" averaged over 35–15°S, 155°E–180°. The sign of each parameter associated with more active Atlantic hurricane seasons is noted in parentheses. Ranks in parentheses represent the 95% confidence intervals for each rank.

Statistic	April-May North Atlantic SST (+)	May Subtropical Atlantic SLP (-)	Tropical Pacific 10m U (-)	April-May Coral Sea SST (+)
1933 Standardized Value	+2.5	-0.3	-1.0	+1.3
1933 Rank (1878-1933)	2	27 (15–37)	11 (3–30)	10
1933 Rank (1878-2015)	20	44 (23–78)	67 (37–104)	58
1878–1932 Correlation w/ ACE	**0.44**	**-0.52**	-0.11	**0.28**
1934–1965 Correlation w/ ACE	0.01	0.20	-0.32	-0.08
1966–2015 Correlation w/ ACE	**0.46**	**-0.27**	**-0.28**	**0.38**

43

Table 5: As in Table 3 but for the current early August statistical hurricane forecast model (Klotzbach et al. 2020b). The three predictors are July 10m "Caribbean Surface" zonal wind averaged over 10–17.5°N, 85–60°W, July SST "Subtropical Atlantic" SST averaged over 20–40°N, 35–15°W and July 200 hPa "Africa Upper-Level" zonal wind averaged over 5–15°N, 0–40°E. The sign of each parameter associated with more active Atlantic hurricane seasons is noted in parentheses. Ranks in parentheses represent the 95% confidence intervals for each rank.

Statistic	July Caribbean Surface Zonal Wind (+)	July Subtropical Atlantic SST (+)	July Tropical Africa Upper-Level Zonal Wind (-)
1933 Standardized Value	+1.7	+1.2	-1.0
1933 Rank (1878-1933)	11 (4–20)	10	9 (1–36)
1933 Rank (1878-2015)	13 (4–34)	47	27 (5–96)
1878–1932 Correlation w/ ACE	**0.51**	**0.50**	-0.10
1934–1965 Correlation w/ ACE	0.26	0.04	-0.10
1966–2015 Correlation w/ ACE	**0.64**	**0.39**	-0.22
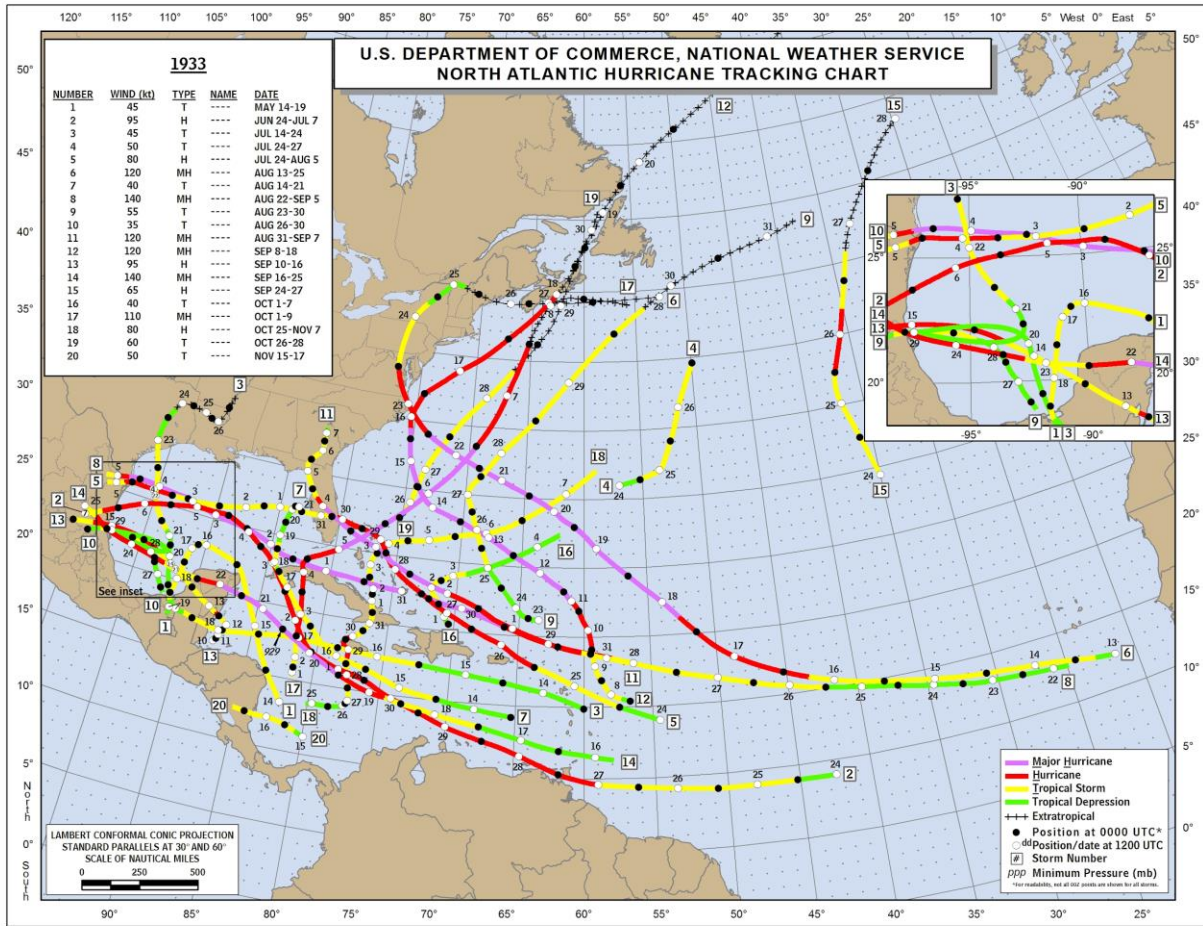
Fig. 1. Tracks of Atlantic tropical cyclones in 1933. Colors indicate storm intensity, with warmer colors denoting a stronger storm. Boxed numbers refer to the storm number as noted in Table 2. Figure courtesy of the National Hurricane Center (https://www.nhc.noaa.gov/data/tracks/tracks-at-1933.png).
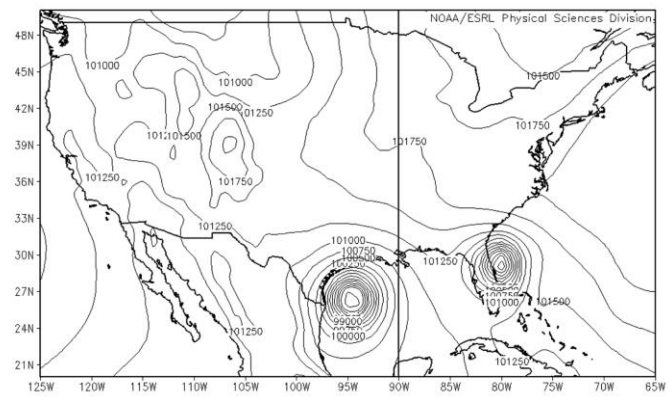
45
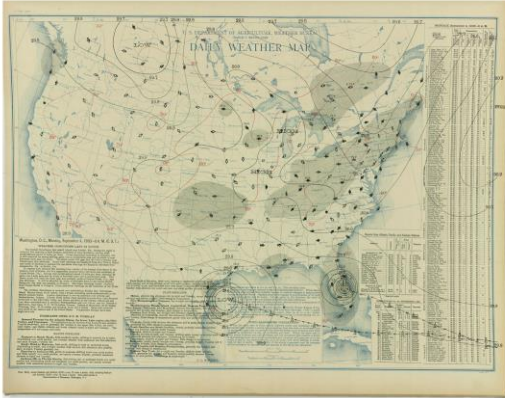
Fig. 2. (a) Daily weather map from the US Weather Bureau on September 4, 1933 at 8am EST

(ftp://ftp.library.noaa.gov/docs.lib/htdocs/rescue/dwm/1933/19330904.pdf) and (b) 20CRv3

MSLP analysis on September 4, 1933 at 12 UTC (one hour earlier than Fig. 2a) .

46
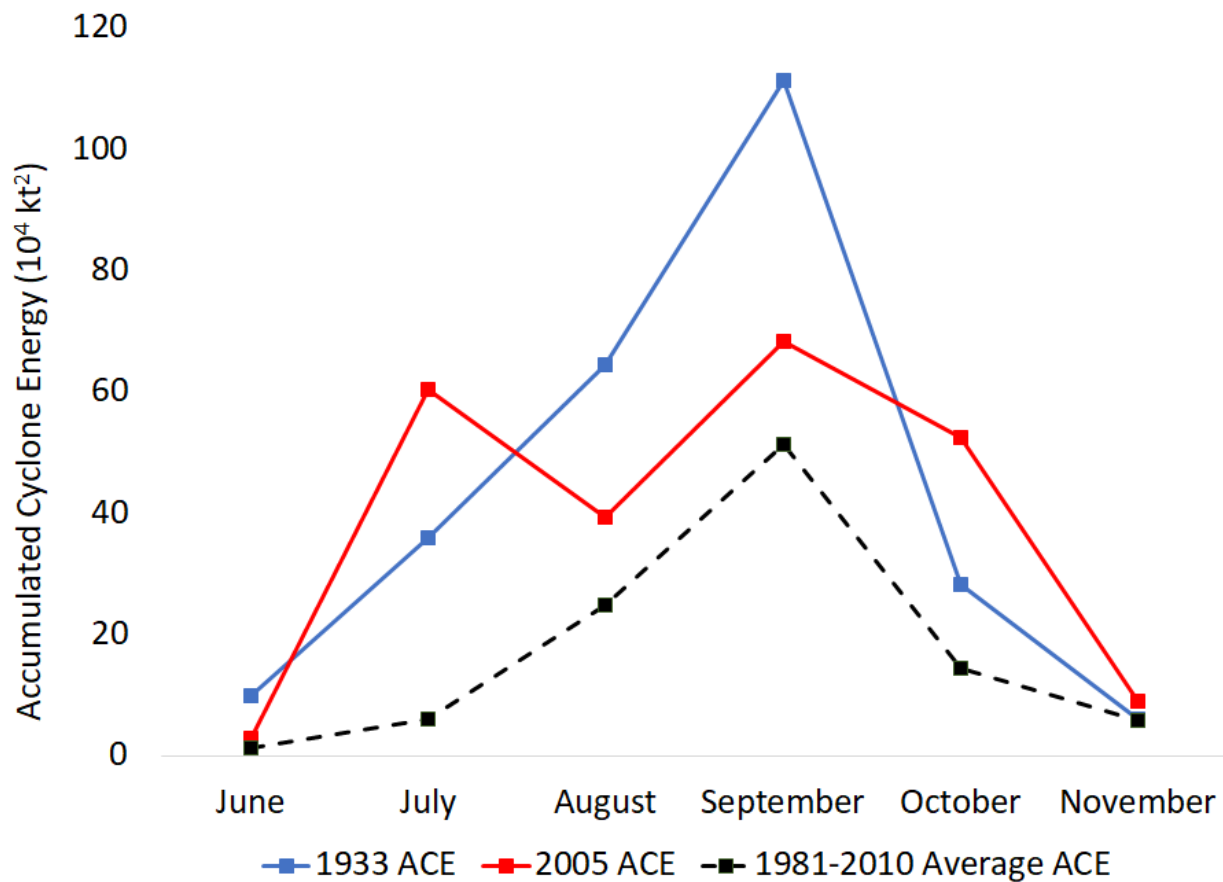
Fig. 3. Accumulated Cyclone Energy by month during the Atlantic hurricane season in 1933 (blue line), 2005 (red line) and the 1981–2010 average (dashed black line).

47
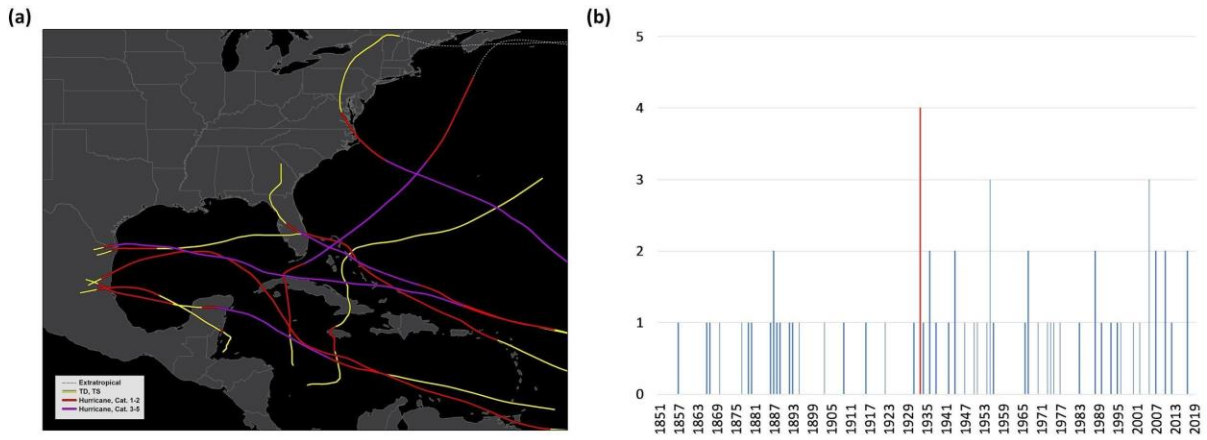
Fig. 4. (a) Tracks of all Atlantic named storms in 1933 making landfall at hurricane strength. (b) Atlantic hurricane landfalls in Mexico since 1851. The number of hurricanes making landfall in Mexico in 1933 is highlighted in red.

48
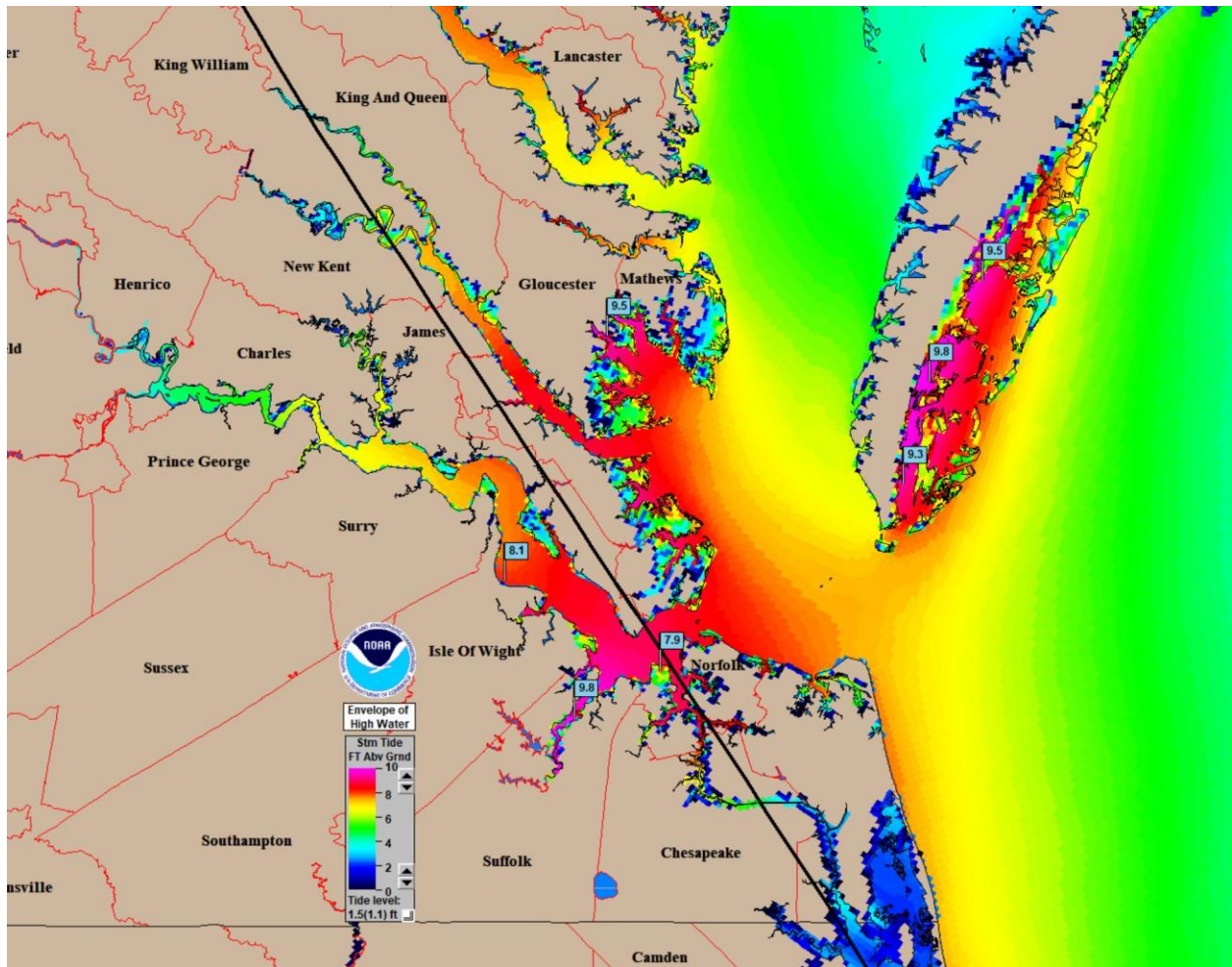
Fig. 5. Storm tide hindcast from the SLOSH model for southeast Virginia from the Chesapeake-Potomac hurricane. The black line denotes the track of the Chesapeake-Potomac hurricane through southeast Virginia.

49
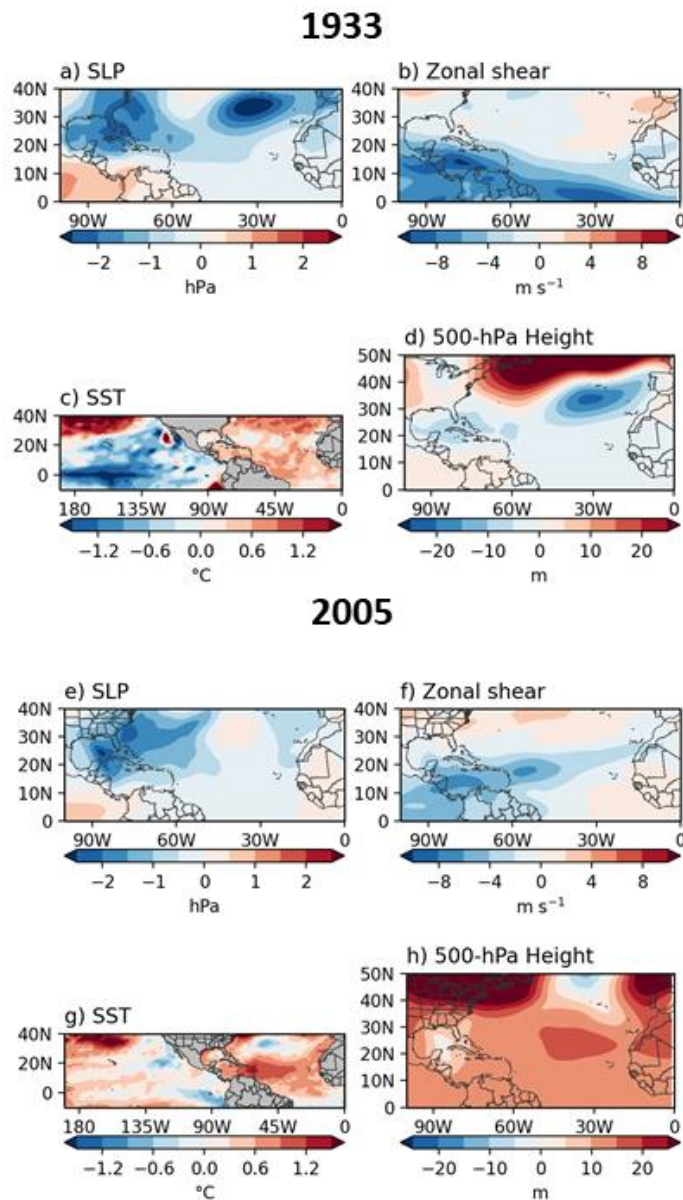
1933

Fig. 6. (a) August–October 1933 sea level pressure anomalies (hPa), (b) August–October 1933 zonal wind shear anomalies (m s^{-1}), (c) August–October 1933 SST anomalies (°C) and (d) August–October 1933 500 hPa geopotential height anomalies (m). (e-h) As in (a-d) but for August–October 2005. Anomalies in panels a–d are calculated relative to a 1901–1930 base period, while anomalies in panels e–h are calculated relative to a 1971–2000 base period.
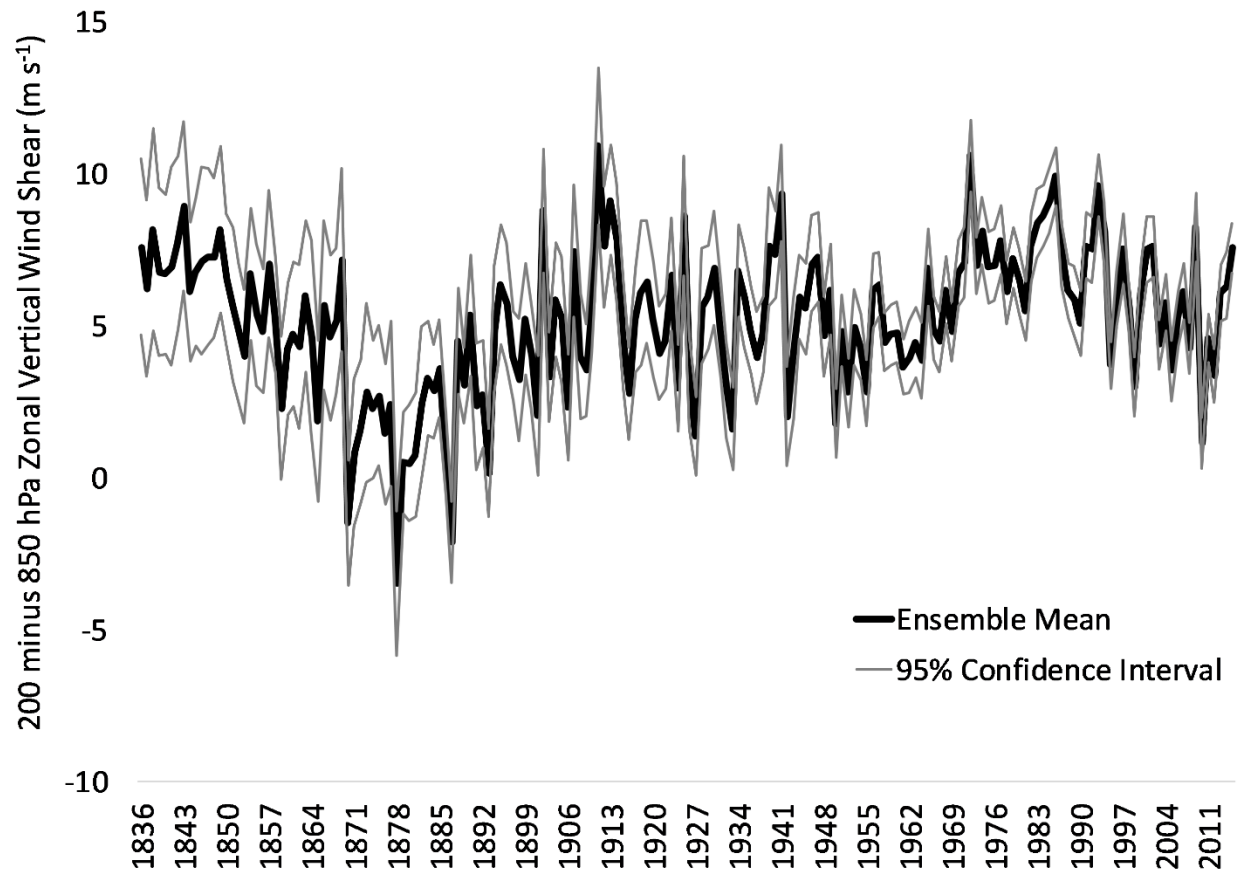
50

Fig. 7. Ensemble mean (thick black line) August–October-averaged 200 minus 850 hPa zonal vertical wind shear (in m s^{-1}) averaged over the MDR from 1836–2015. Negative values indicate easterly shear. 95% confidence intervals are also plotted (thin gray lines).
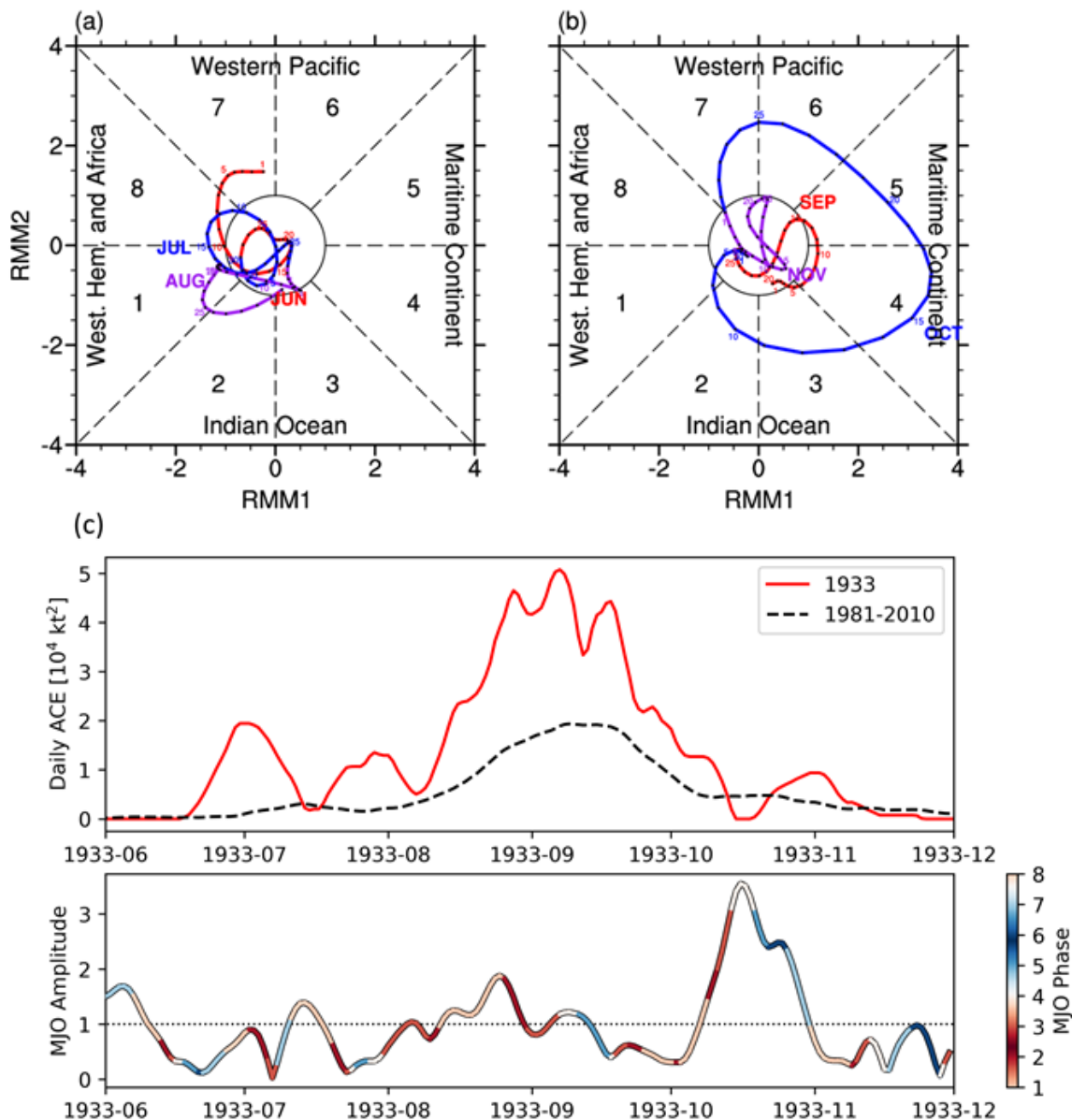
Fig. 8. (a) MJO index propagation from June 1 – August 31, 1933. (b) MJO index propagation from September 1 – November 30, 1933. (c) (top panel) Daily ACE from June 1 – November 30, 1933 with a 15-day smoothing applied. The date plotted is the midpoint of the 15-day period being averaged. (c) (bottom panel) Daily MJO amplitude from June 1 – November 30, 1933. Warmer colors indicate phases of the MJO typically associated with more active Atlantic hurricane periods based on the results of Klotzbach and Oliver (2015a).
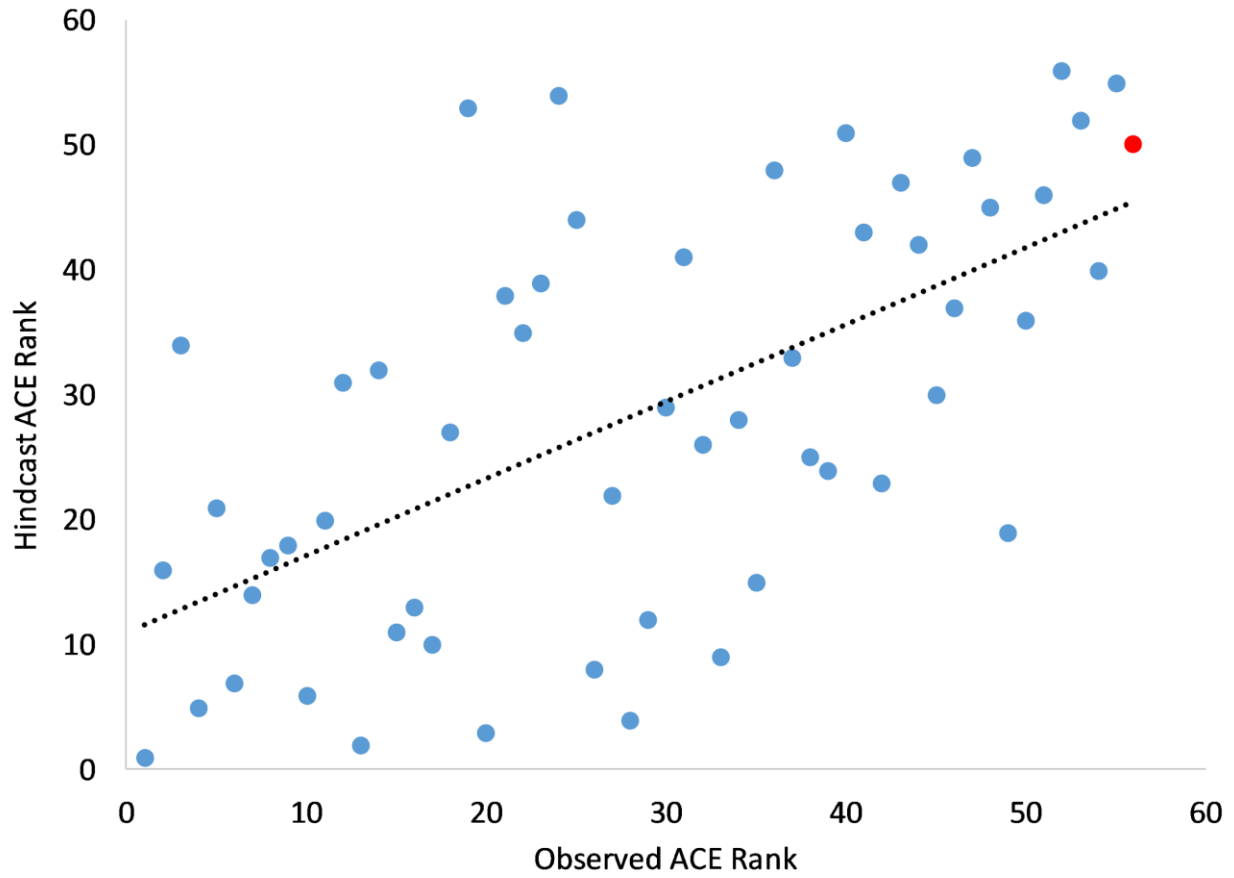
52

Fig. 9. Observed vs. hindcast ACE rank using the early June statistical model from CSU for the period from 1878–1932. Higher ranks indicate higher levels of ACE. The red dot represents the model forecast for the 1933 Atlantic hurricane season.
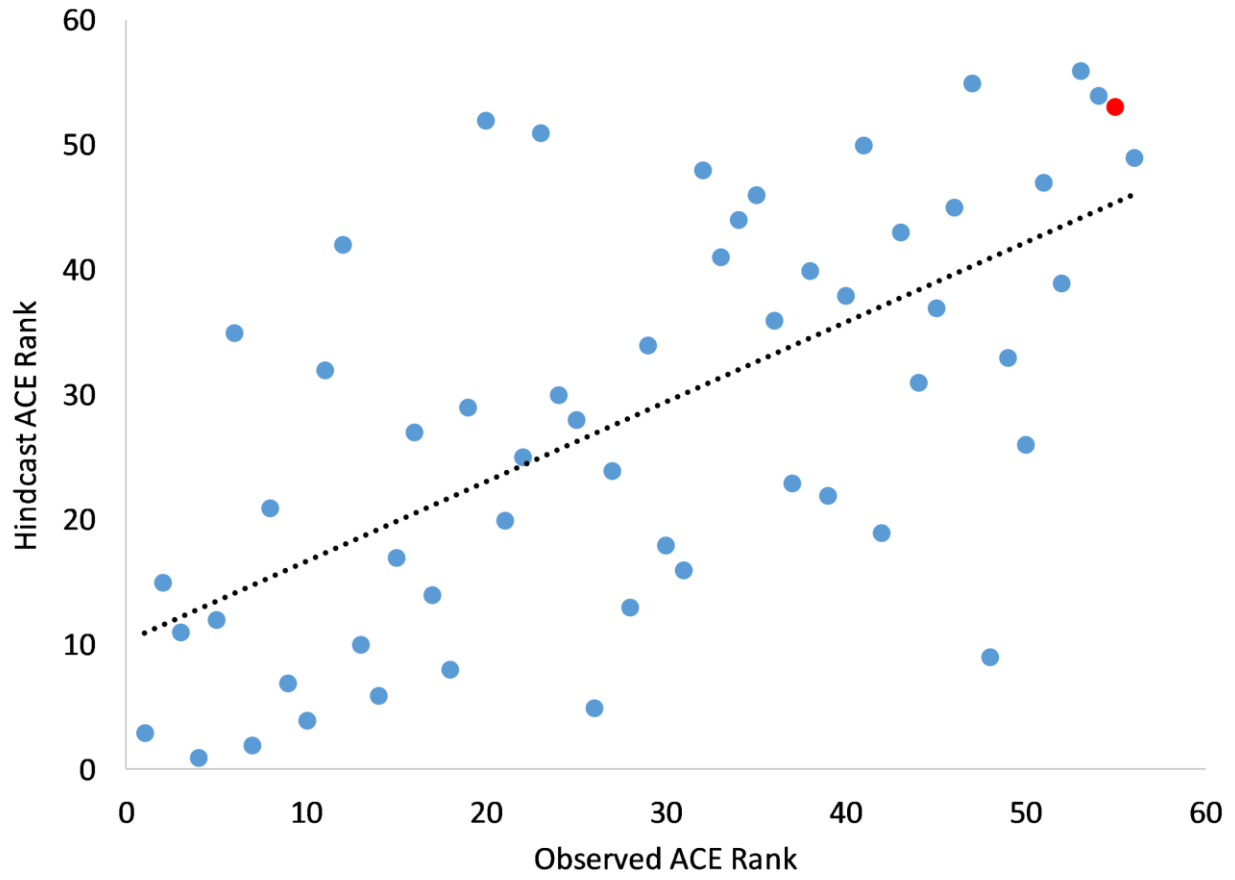
53

Fig. 10. As in Fig. 9 but using the early August statistical model.